Oceanologia 66 (2024) 250—266

Available online at www.sciencedirect.com

ScienceDirect

journal homepage: www.journals.elsevier.com/oceanologia

ORIGINAL RESEARCH ARTICLE

Rapid coastal erosion, its dynamics and cause — an erosional hot spot on the southern Baltic Sea coast

Grzegorz Uścinowicz[a,*], **Szymon Uścinowicz**[b], **Tomasz Szarafin**[a], **Elżbieta Maszloch**[a], **Kamila Wirkus**[a]

[a] *Polish Geological Institute — National Research Institute, Marine Geology Branch, Gdańsk, Poland*
[b] *Institute of Hydro-Engineering, Polish Academy of Sciences, Gdańsk, Poland*

Received 30 January 2023; accepted 14 December 2023
Available online 26 December 2023

KEYWORDS
Nontidal;
Sea ice;
Barrier coast;
Storminess

Abstract Coastal erosion is one of the major problems in coastal management. To adapt to it, and prevent it where possible and needed, it is important to recognize the temporal and spatial scale of the phenomenon as well as its causes. This paper describes the rapid erosion rate along an approximately 2.25 km stretch of the southern Baltic coast. The erosion occurs within a nature reserve, which is not subject to direct anthropogenic impact. Historical maps and modern remote sensing were used to trace changes in the shoreline position from 1875 to the present, and detailed DTMs derived from airborne LiDAR were used to trace elevation changes of the beach and dunes over the past years. The weighted maximum annual erosion rate since 1875 averages 2.3 m. An increase in this annual erosion rate has been observed since the turn of the millennium. The maximum average erosion rate from 2001 to 2005 was 15 m/year. The erosion has caused serious changes in elevation within the inland part of the coastal zone, manifested by a reduction in the width of the beach and a decrease in the height of the beach and dunes.

* Corresponding author at: Polish Geological Institute — National Research Institute, Marine Geology Branch, 5, Kościerska Street, 80-328 Gdańsk, Poland.
E-mail address: grzegorz.uscinowicz@pgi.gov.pl (G. Uścinowicz).
Peer review under the responsibility of the Institute of Oceanology of the Polish Academy of Sciences.

Production and hosting by Elsevier

https://doi.org/10.1016/j.oceano.2023.12.002

1. Introduction

Coastal erosion is a worldwide phenomenon and one of the major problems in coastal management. To adapt to it, and sometimes prevent it, it is important to recognise the temporal and spatial scale of the phenomenon and its causes. Of special interest and importance are the shoreline segments where recession rates are significantly higher than for neighbouring shoreline segments. These areas of erosion anomalies (sensu Galgano, 2007) or so-called "erosional hot spots — EHSs" (sensu Kraus and Galgano, 2001) are a serious problem causing significant losses to coastal areas of high value, including natural habitats, and areas of economic importance such as forests, agricultural land, tourist resorts and residential areas. In general, EHSs are classified according to the duration of existence, lateral extent, processes responsible for the erosion, and predominant erosion mechanism as longshore or cross-shore transport (Kraus and Galgano, 2001). There are a number of natural and anthropogenic factors that cause beaches to erode at anomalous rates (e.g. Benedet et al., 2007; Bridges, 1995; Esteves and Finkl, 1998). Possible natural reasons that cause EHSs are evaluated, i.a. in terms of wave transformation over bathymetric irregularities located both offshore and shoreface, alongshore grain-size distribution, and shoreline orientation. EHSs are also frequently observed in response to human interventions such as the construction of jetties in river mouths or entrances to harbours, as well as to coastal protection structures like groins and seawalls. (Dean et al., 1999; Kraus and Galgano, 2001). The identification and assessment of EHS is crucial for coastal zone management.

Erosion is also a pervasive problem in the Polish coastal zone of the southern Baltic Sea. Studies of Polish coasts have a long tradition (Furmańczyk, 1994; Furmańczyk and Musielak, 1999, 2002; Musielak et al., 2017; Zawadzka, 1999, 2012; Zawadzka-Kahlau, 1999), however, they have mostly been limited to tracking changes in the position of the coastline. More valuable explanatory research focused on identifying coastal sections particularly affected by erosion, and attempting to determine the causes of erosion, were mainly limited to cliff coasts and were mainly published in Polish journals (Subotowicz, 1991; Uścinowicz et al., 2004). Studies focused on the identification of EHSs in relation to barriers along the Polish coast and cause-effect analyses of temporal changes in the rate of erosion are extremely rare.

This paper describes the spatial and temporal characteristics of a recently identified EHS that has modified an uninterrupted sandy coast completely free of human intervention. We present a case study of one of the most severely eroded sections of the Polish coast, tracking the range of coastal erosion and specifically changes in the erosion rates to define and understand EHS. In particular, we seek to answer the following questions:

1) How fast annually the coastal retreat can be,
2) How and why the rate of coastal erosion has changed,
3) If the location of the EHS is stable or changes over time and space,
4) What causes anomalously rapid local coastal erosion.

2. Regional setting

The Polish coast of the Baltic Sea has a total length of 498 km (without internal lagoonal coasts). The coastal zone, as central and northern Poland, is dominated by Pleistocene glacial and glaciofluvial deposits. In terms of morphology and geological structure, three types of coasts are distinguished: cliffs (ca. 101 km), barriers (ca. 380 km) and coasts similar to wetlands (ca. 17 km). The entire southern Baltic coast has been subject to erosion processes for centuries. Most of the cliffs have been affected by significant levels of erosion (Subotowicz, 1995; Terefenko et al., 2019; Uścinowicz et al., 2017). Behavioural changes taking place along the barrier coast are more complex. Most barriers are eroded to varying degrees and rates (Deng et al., 2017; Zawadzka, 2012), but unlike cliffs, they can recover and build seaward. A minor part of the Polish barrier coast is relatively stable or aggrading. While analysing changes in the location of the coastline on a decadal time scale, erosion-accumulation systems of different spatial scales were identified, with the predominance of erosion processes (Zawadzka, 1999). The average rate of shoreline retreat within the erosive sections was about 0.5—2 m/year, depending on the location and period of measurements (Meier et al., 2022; Michałowska and Głowienka, 2022; Zawadzka, 1999).

The study area extends from east to west along an approximately 5.5 km stretch of barrier coastline between 17°49′16″ and 18°23′12″E, between the villages of Dębki and Karwia. According to the state coastline division system for the Polish coast, it stretches between km 142.5 and km 148 (Figure 1). The area has been affected by rapid coastal erosion during the past decades. The marine part of the site is entirely within a Natura 2000 Special Area of Conservation (PLB990002 — Przybrzeżne Wody Bałtyku). The land part of the area is partly within the Coastal Landscape Park and, at the same time, within the Widowo Nature Reserve (Habitat Site PLH220054). The study area can be considered as an area where coastal processes are not directly disturbed by anthropogenic factors. Beach nourishment and the nearest breakwaters disturbing the longshore sand transport are located in Łeba, ca. 40 km west of the study area. To the east of the study area, an embankment has been constructed along a stretch of approximately 2 km to protect the foredune and coastal lowland against storm surge flooding.

The Baltic Sea is an intracontinental, semi-enclosed, brackish and non-tidal sea. The climate of the Baltic Sea region is influenced by the large-scale atmospheric circulation and shows a strong seasonal cycle, but also large interannual to multidecadal variability. There are no significant long-term trends in wind speed and direction, but there is considerable decadal variability. Correspondingly, there are no clear indications of long-term trends in the frequency of storm surges and wave height (Bärring and Fortuniak, 2009; Climate Change in the Baltic Sea, 2021; HELCOM, 2007, 2013; Rutgersson et al., 2014).

In general, westerly winds dominate over the southern Baltic Sea region. Typically, the highest wind speeds are associated with the passage of strong extratropical cyclones. These systems, and thus wind extremes, are most frequent and intense in the winter season. The wave climate in the

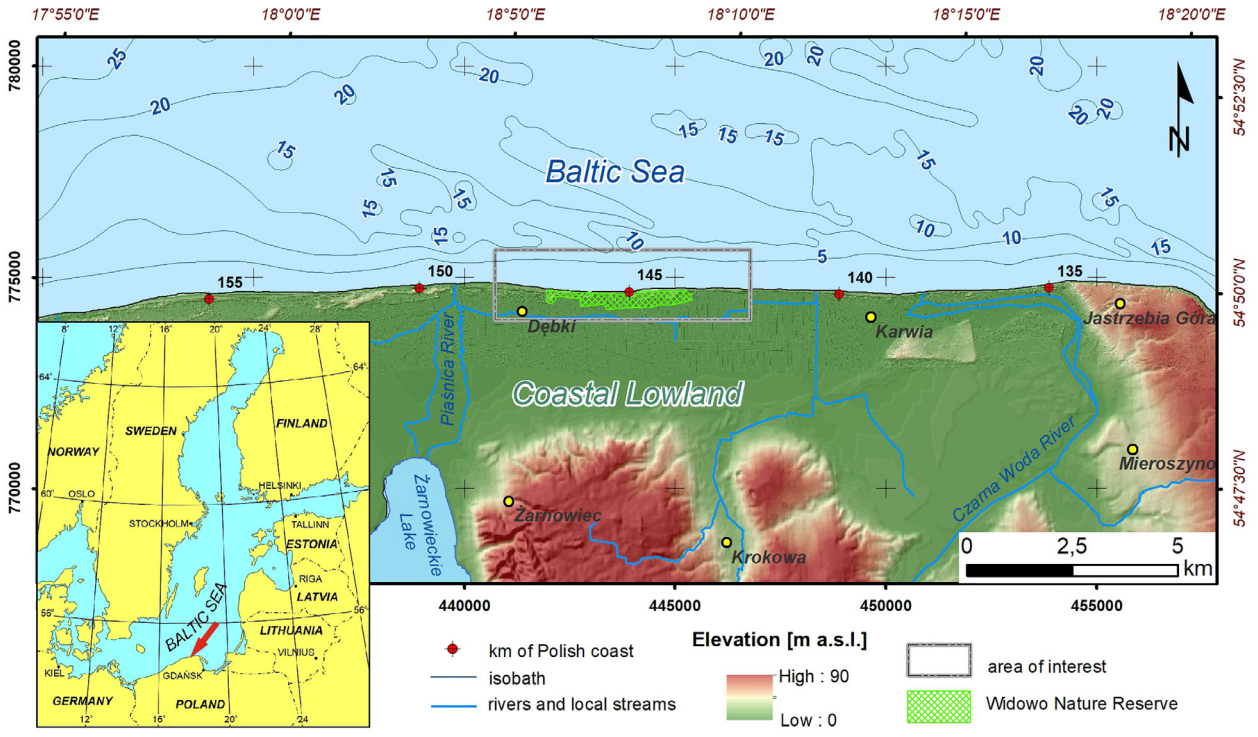

Figure 1 Location of the study area. Source of bathymetry — Polish Geological Institute — National Research Institute; source of DTMs — Maritime Office in Gdynia and Military Centre of Geodesy and Remote Sensing, and IT system for the Country's Protection Against Extreme Hazards (ISOK).

Baltic Sea strongly depends on the wind field, and consequently, waves from the western sector (SW, W, NW) dominate. Representative wave data for the study area are derived from the Coastal Research Station of the Institute of Hydro-Engineering of the Polish Academy of Sciences in Lubiatowo, located ca. 18 km to the west (Ostrowski et al., 2016). Waves from the western sector occur for ca. 50% of the year, more than from the eastern sector (NE, E, SE — 32%) and the northern sector (13.5% of the year). Storm winds (> 15 m/s) and waves also mostly come from SW, W and NW. During heavy storms, the parameters of deep-water waves may exceed: $H_{max} > 7$ m, $H_s > 4$ m, $H_{mean} > 3$ m, $T_s > 9$ s, $T_{mean} > 8$ s. Owing to the existence of sandbars, most of the wave energy is dissipated when approaching the shore (Pruszak et al., 2011). In storm conditions, however, return currents in the surf zone reach velocities of up to 0.5 m/s, while the greatest velocities of longshore currents reach 1.2—1.5 m/s. Driven by longshore currents, the annual resultant (net) longshore sediment transport on the shoreface (in the zone up to 650 m from the shore) is ca. 111,000—145,000 m^3/year, directed from west to east (Szmytkiewicz et al., 2021).

In general, the sea level is rising along the entire southern Baltic coast. According to the nearest mareographic station located in Władysławowo, ca. 20 km east of the study area, the average rate of water-level rise in the period 1951—2015 was 2.04 mm/year (Kowalczyk, 2019). In addition to long-term water-level rise, there are also sudden events when extremely high water level reaches of about 1.5 m above m.s.l. (mean sea level) within a few hours, during the migration of low-pressure storm systems. The maximum recorded water level in Władysławowo was 1.38 m above m.s.l. (Wiśniewski et al., 2009).

Morphologically, the coast in the area of interest is dissipative, with multiple nearshore bars and a lowland in the hinterland. The surface of this lowland is at 0.7—1.5 m a.s.l. and is cut by a network of drainage ditches. The barrier separating the lowland from the sea is relatively narrow and low. The width of the beach is 40—50 m in summer and is reduced to 10—20 m during autumn and winter storms. A strip of morphologically variable dunes extends landward beyond the beach. A 3—5 m high foredune occurs only in the western and eastern parts of the study area. The middle section, ca. 2 km long, is heavily eroded, so there is no foredune. Directly adjacent to the beach are dunes up to about 20 m high, which are erosional remnant of parabolic dunes (Figure 2).

The shoreface (underwater coastal slope) reaches a width of 1.0—1.3 km and an has average inclination of ca. 1:100. In the upper part of the shoreface, up to a depth of 5—6 m b.s.l. (below sea level), there are two to three low sandbars with a crest-to-trough amplitude of 0.5—2.5 m. The first sandbar, closest to shore, is usually a highly eroded form, i.e. faintly defined and merging with the beach. The second sandbar is more clearly defined along the length of the shore. Located at a distance of ca. 150—200 m from shore, it is semi-permanent and mostly continuous. The third sandbar, approximately 400—500 m from shore, is fragmented in places and transitions into a slightly inclined to the north sandy flat. This plain forms the lower shoreface and extends to an approximate depth of 10—12 m b.s.l. The shoreface at a depth of ca. 10—12 m b.s.l. is marked by

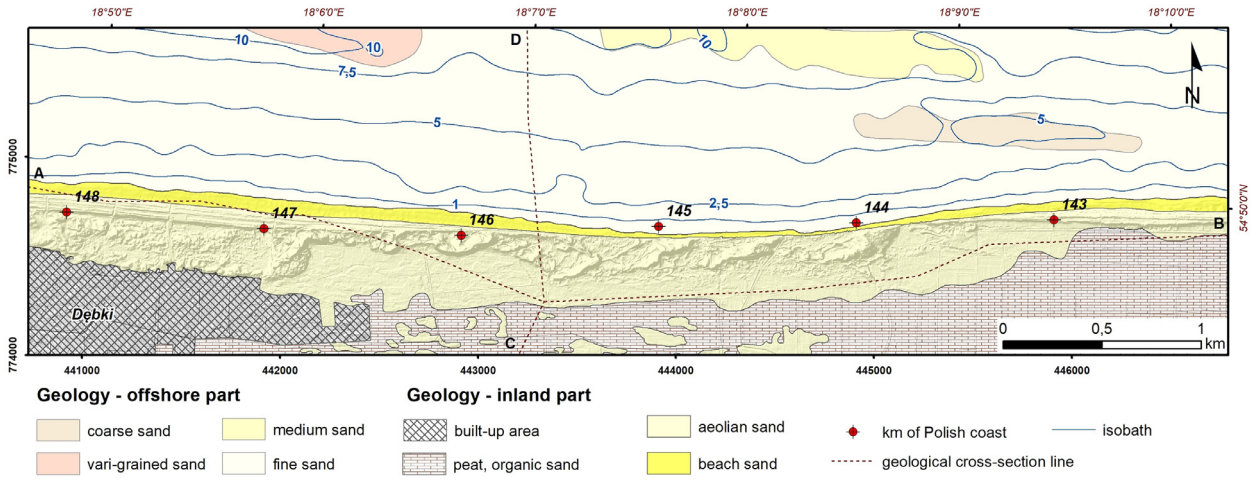

Figure 2 Geological map of the study area (Polish Geological Institute — National Research Institute materials).

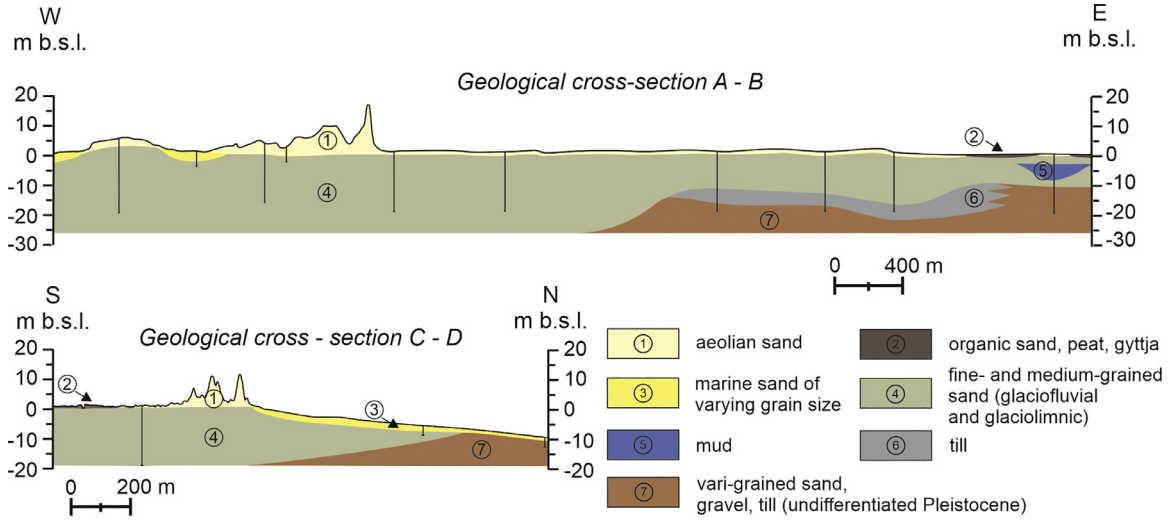

Figure 3 Geological cross-sections through the study area. The cross-section lines are shown in Figure 2 (Polish Geological Institute — National Research Institute materials).

a gradient change. In the northern part of the study area, seaward of the sandy plain at a depth of 12—20 m, there are shoreface-connected ridges with a depression between them. The axis of this swale is NW-SE oriented, i.e. obliquely towards the shore.

The onshore subsurface of the study area is composed of Quaternary formations with a thickness of ca. 40—50 m and consists mainly of a Pleistocene sequence of sand of glaciofluvial and glaciolimnic origin and till. Holocene peat with a thickness of up to 1.5 m forms the surface of the lowland (Figures 2 and 3). Thin layers of storm surge deposits (Moskalewicz D., 2016) and/or aeolian sands interfinger with the peat at the barrier-lowland transition zone (Uścinowicz et al., 2021).

As for the marine subsurface of the study area, the topmost part of the Pleistocene deposits was partly eroded during the Holocene marine transgression. Despite this truncation, the geological structure of the Pleistocene deposits is similar to its terrestrial equivalent. The overlying Holocene deposits are dominated by marine sand and, locally, gravel. The thickness of marine sediments ranges from a few cm to 3—4 m (Uścinowicz et al., 2018). The largest thickness occurs within the sandbars and sand ridges. These landforms are composed of medium and fine sand with *Macoma* sp. shells and fragments of shells. In the depressions of the seabed between the sandbars and between the sand ridges, coarse-grained sand, locally with gravel admixture, occurs. Here, the thickness of marine sediments is locally reduced to a few centimetres.

3. Material and methods

An extensive remote sensing analysis was carried out for the study area, comparing multi-temporal digital elevation models and tracking changes in the position of the shoreline in relation to the oldest available and processed cartographic materials. The unquestionable advantage of this method is the possibility of quantifying changes over different periods. The following materials were used for this

analysis: (1) LiDAR data acquired by airborne laser scanning performed as part of coastal monitoring by the Maritime Office in Gdynia; (2) geoprocessed maps, aerial photos, DEMs and shorelines established/generated from these products that each represent the situation for a specific time.

According to the Maritime Office report, the airborne LiDAR mapping was designed to have at least one flight profile over water, so that the LiDAR beam could scan the northern side of dune slopes. The survey was carried out with the water level not exceeding 10 cm above m.s.l. The average scanning density was 8 points/m^2 and the overlap between areas covered with LiDAR beam was at least 20%. The total width of the mapped coastal zone was about 0.5 km.

Multi-temporal digital elevation model was developed to show changes in the topography of the coastal zone between 2016 and 2020. Individual digital elevation models have an average z (vertical) value inaccuracy of about 0.15 m. A series of control points were selected to check height differences between the individual DEMs to minimize the error in z-values on the final multi-temporal model. The maximum inaccuracy of two DEMs varied and ranged from 0.05 to 0.35 m.

The uniformity of the DEMs output allowed the comparison of models created based on different measurement series at different times. This methodological approach allowed vertical changes to be quantified. For the purpose of the analysis, the vertical changes between −0.5 and 0.5 m were classified as the "stable" state (gray), with positive values (two classes 0.5–2 m and 2–5 m) corresponding to an increase in the height of the measured areas (green) and negative values (two classes −0.5– −2 m and −2– −5 m) corresponding to a decrease in height (red). The obtained multi-temporal model provides information about the vertical changes that occur in individual coastal sections and facilitates the general parameterisation of these changes.

A second indicator of coastal change, shoreline migration, can be analysed for a longer time horizon. The 1875 shoreline generated from a geoprocessed, German archival topographic map (Topographische Karte, Messtischblatt 1:25,000, 136-Dembek) was compared with those from 1958, 1980, 2001, 2005, 2010, 2016 and 2020 (Table 1). The Messtischblatt maps are characterised by a high level of accuracy, reaching up to 4–6 m compared to modern cartographic materials (Deng et al., 2017). The shoreline on modern topographic maps (1980, 2001 – a year of the cartographic survey) is a linear feature with a width of approximately 0.5 mm. The position of the shoreline was GIS-digitized directly from the official cartographic materials. This methodological approach permits an accuracy of a few metres and ultimately up to 10 m, which depends on the accuracy of the original map. A similar procedure was applied to orthophotomaps (1958, 2005) and ultimately the fitting accuracy can be estimated at a level of 5 m, which in this case depended on the resolution and pixel size of the original photo. With regard to the DEMs, the shoreline was 0 m above sea level. The validity of this procedure was verified by comparing the shoreline derived from an orthophotomap taken at the same time. The shoreline position derived from the DEMs has an accuracy of 5 m, resulting from the original DEMs resolution. For technical reasons (the shoreline merges to the map frame), it was not possible to determine

Table 1 List of materials used in the study.

Type of source data	Year	Typ of analysis	Data source	Estimated lateral error or pixel size
DTM	2016	Multi-temporal DTM	Maritime Office in Gdynia	0.5 m – pixel size
DTM	2020	Multi-temporal DTM	Maritime Office in Gdynia	0.5 m – pixel size
Topographic map – Messtichblatte 1: 25 000	1875	shoreline position	PGI-NRI (derived from topographic map)	25 meters (Deng et al., 2017)
Aerial photo (orthophotomap)	1958	shoreline position	PGI-NRI (derived from aerial photo)	<5 m
Topographic map 1: 10 000	1980	shoreline position	PGI-NRI (derived from topographic map)	<10 m – map accuracy
Topographic map 1: 10 000	2001	shoreline position	PGI-NRI (derived from topographic map)	<10 m – map accuracy
Aerial photo (orthophotomap)	2005	shoreline position	PGI-NRI (derived from aerial photo)	2.0 m – pixel size
DTM	2010	shoreline position	PGI-NRI (derived from DTM)	0.5 m – pixel size
DTM	2016	shoreline position	PGI-NRI (derived from DTM)	0.5 m – pixel size
DTM	2020	shoreline position	PGI-NRI (derived from DTM)	0.5 m – pixel size

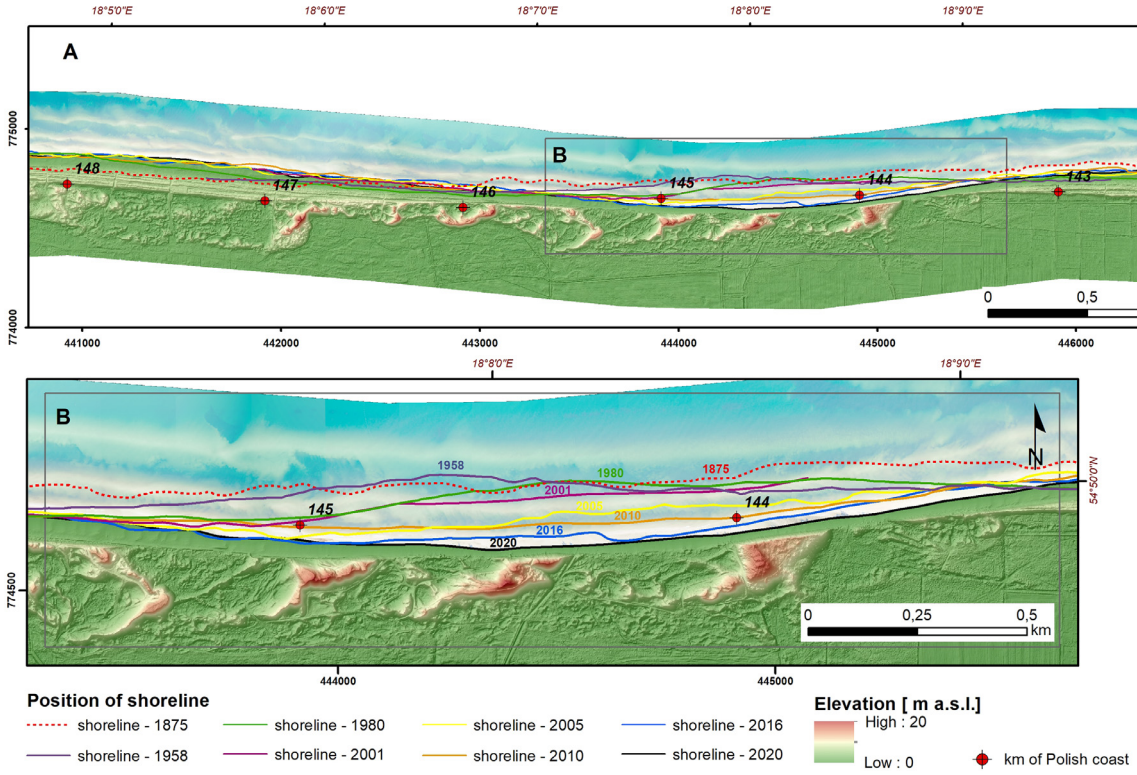

Figure 4 Shoreline position changes.

the position of the shoreline in 2001 in the vicinity of km 142—144 (the eastern part of the study area).

Additionally, to compare peak values of shoreline changes over time, the areas of erosion and accretion were calculated. For this purpose, the study area was divided into three sections bordered by "nodal points" corresponding to the EHS and adjacent areas. In these sections, the area bounded by the two respective shorelines was measured. Each created polygon was classified as either an area of erosion or accumulation depending on the layout of the boundary lines. The total area of erosion and accumulation in each section was then counted. In cases where the full course of shoreline was not available (due to lack of data) in a given section, polygons were created only based on the part covered by the common range. In this case, the results obtained should be regarded as minimum values. The data prepared in this way were used to calculate the average longshore erosion/accretion. This was achieved by dividing the respective area of erosion/accretion by the corresponding length of the shoreline.

4. Results

The general trend in changes of the coastal zone was analysed by comparing the changes in the erosion/accretion areas and position of the shoreline in 1875, 1958,1980, 2001, 2005, 2010, 2016 and 2020 (Figure 4). The oldest analysed shoreline in the study area, i.e. the shoreline from 1875, is located mainly in the present sea area and encroaches on land at km 142.6 and 146.0 of the Polish coast. Only in a small, 0.5-km-long section (between km 144.45 and 144.95), is the 1958 shoreline located slightly (at most about 36 m) seaward of the 1875 shoreline. Even younger shorelines are located landward, but still in the sea area. They cross the present-day shoreline between km 143.4—143.7 to the east and km 145.3—145.6 to the west of the EHS. The strongest erosion occurred within a 2.2-km-long section between km 143.4 and 145.6 (Figure 4). The maximum shoreline retreat within this section was about 150 m between 1875 and 2020 and about 170 m between 1958 and 2020. As a result, a concave erosional section of ca. 3.4 km has been forming since at least 1875 (Figure 4). Owing to its large scale and high rate of erosion, it can be classified as an EHS (*sensu* Kraus and Galgano, 2001). When analysing in more detail the changes in the location of the shorelines within the hot spot over different periods, a large variability in the areas of erosion/accretion, range and rate of shoreline displacement was found, with erosion by far the dominant factor (Tables 2—4 and Figure 4). Between 1875 and 1958, the shoreline mostly shifted landward by an average of 25 m at an average rate of up to 0.3 m/year; only locally, in a 0.5-km section, it shifted seaward by a maximum of 36 m. The peak values and average peak rate were respectively 64 m and 0.8 m/yr. Next, in the period 1958—1980, the shoreline retreated by an average of 14 m (peak value of 64 m) with a corresponding average rate of 0.6 m/yr (peak rate increasing to 2.9 m/yr), but there were also short sections where the shoreline shifted seaward by up to 25 m.

Since 1980, no local accumulation has been recorded within the hot spot, while erosion clearly accelerated at the turn of the millennium. Between 1980 and 2001, the shoreline shifted at an average 14 m (peak value up to 33

Table 2 Shoreline position changes within the erosional hot spot and boundary areas.

Period	Shoreline position changes within the western boundary area (west of km 145.600)	Shoreline position changes within the "erosional hot spot" (km 143.4—145.6 km)	Shoreline position changes within the eastern boundary area (east of km 143.4)
1875—1958	local state of equilibrium **erosion up to ca. 70 m** accretion up to ca. 30 m	local state of equilibrium **mostly erosion up to ca. 64 m** local accretion up to ca. 36 m	**erosion up to ca. 95 m**
1958—1980	**erosion up to ca. 22 m**	local state of equilibrium **mostly erosion up to ca. 64 m** local accretion up to ca. 25 m	**accretion up to ca. 21 m**
1980—2001	**accretion up to ca. 50 m**	**erosion up to ca. 33 m** local state of equilibrium	lack of data
2001—2005	local state of equilibrium local erosion up to ca. 20 m local accretion up to ca. 25 m	**erosion up to ca. 61 m**	lack of data
2005—2010	local state of equilibrium local erosion up to ca. 29 m local accretion up to ca. 43 m	local state of equilibrium **mostly erosion up to ca. 33 m** local accretion up to ca. 26 m	local state of equilibrium local erosion up to ca. 20 m local accretion up to ca. 40 m
2010—2016	local state of equilibrium local erosion up to ca. 28 m local accretion up to ca. 37 m	**erosion up to ca. 42** local state of equilibrium	local state of equilibrium local erosion up to ca. 15 m local accretion up to ca. 37 m
2016—2020	local state of equilibrium local erosion up to ca. 33 m local accretion up to ca. 26 m	**erosion up to ca. 31 m** local state of equilibrium	local state of equilibrium local erosion up to ca. 13 m local accretion up to ca. 10 m

m landward), but the average rate was still relatively slow at about 0.7 m/yr (peak rate 1.6 m/yr), whereas between 2001 and 2005 the average retreat reached 31 m (up to 61 m), at a rate of 7.7 m/yr (peak average of 15.3 m/yr!). In the period 2005—2010, the position of the shoreline generally retreated by an average of 6 m (peak value up to 33 m), corresponding to an average rate of 1.1 m/yr and maximum rate of 6.6 m/yr, and locally shifted seaward by a maximum of 26 m. After this period of a relatively slower rate of shoreline retreat, the process of erosion accelerated again. This manifested itself in average shoreline retreat across the erosional hot spot by approximately 21 m (peak value up to 42 m) in the period 2010—2016 and a further average of 13 m (maximum 31 m) in the period 2016—2020 at average rates 3.5 and 3.2 m/yr, respectively (maximum rates of 7.0 and 7.8 m/yr) (Tables 2 and 3, Figure 4).

Transformation within the EHS can also be reflected by changes in the area undergoing erosion or accumulation (Tables 3 and 4). These changes correlate very well with the phenomena described above and are based on the analysis of the position of the shorelines. Based on an analysis of the area subject to net erosion, it can be assumed that 54 591 m^2 were lost between 1875 and 1958. This results in an average loss of 658 m^2/year. Between 1958 and 1980, a further 30 942 m^2 (1 406 m^2/year) was eroded within the EHS. In the next analysed period (1980—2001), these values decreased and amounted to 24 574 m^2 (1 170 m^2/year), only to increase again at the turn of the century, i.e. between 2001 and 2005, amounting to 55 744 m^2 (13 936 m^2/year). The period from 2005 to 2010 saw a repeated decrease in erosion (12 441 m^2; 2 488 m^2/year). Conversely, the following years 2010— 2016 and 2016— 2020 show a renewed increase in land loss, 45 818 m^2 and 28 467 m^2 (7 636 m^2/year and 7 117 m^2/year, respectively).

The range of changes on both sides of the erosional hot spot was much smaller, but more variable in terms of behaviour. East of the erosional hot spot, i.e. east of km 143.4, the shoreline moved landward by an average of 29 m and a maximum of about 95 m between 1875 and 1958. During the next measurement period 1958—1980, erosion slowed down and even reversed to accretion in some places, with the shoreline shifting seaward by an average of 4 m (up to 21 m). Unfortunately, it was not possible to describe the changes between 1980 and 2001 for this coastline section. Between 2005 and 2010, the position of the shoreline moved generally landward by an average value of 5 m and a maximum of approximately 20 m and locally shifted seaward by an average of 13 m (up to 40 m). Between 2010 and 2016, the changes were similar, varying between a local retreat (average of 7 m and up to approximately 15 m) and a local seaward shift (average of 10 m and maximum measured 37 m). Between 2016 and 2020, the position of the shoreline changed only slightly and oscillated between a local seaward or landward shift. Therefore, the period from 2005

Table 3 Area of erosion/accretion changes within the erosional hot spot and boundary areas.

Period	Area of erosion/accretion changes within the western boundary area (west of km 145.6)			Area of erosion/accretion changes within the "erosional hot spot" (143.4–145.6 km)			Area of erosion/accretion changes within the eastern boundary area (east of km 143.4)		
	Dominant process	Total area [m^2]	Longshore average erosion (total area/length of shoreline) [m]	Dominant process	Total area [m^2]	Longshore average erosion (total area/length of shoreline) [m]	Dominant process	Total area [m^2]	Longshore average erosion (total area/length of shoreline) [m]
1875–1958	**erosion***	**30163**	**20**	**erosion**	63643	**29**	**erosion***	43823	**29**
	accretion*	8768	6	accretion	9052	4	accretion*	0	0
1958–1980	**erosion***	**19642**	**13**	**erosion**	44729	**20**	erosion*	118	0
	accretion*	6706	4	accretion	13787	6	**accretion***	5370	**4**
1980–2001	erosion*	0	0	**erosion****	24867	**14**	lack of data	lack of data	lack of data
	accretion*	**48547**	**32**	accretion**	293	0			
2001–2005	erosion*	1585	1	**erosion****	57043	**32**	lack of data	lack of data	lack of data
	accretion*	**10638**	**7**	accretion**	1299	1			
2005–2010	**erosion**	**21444**	**9**	**erosion**	22964	**10**	erosion	4606	5
	accretion	17180	7	accretion	10523	5	**accretion**	11920	13
2010–2016	erosion	10782	4	**erosion**	46637	**21**	erosion	6723	7
	accretion	**25627**	**11**	accretion	819	0	**accretion**	9183	10
2016–2020	**erosion**	**23234**	**10**	**erosion**	30867	**14**	**erosion**	6264	7
	accretion	7161	3	accretion	2400	1	accretion	1784	2

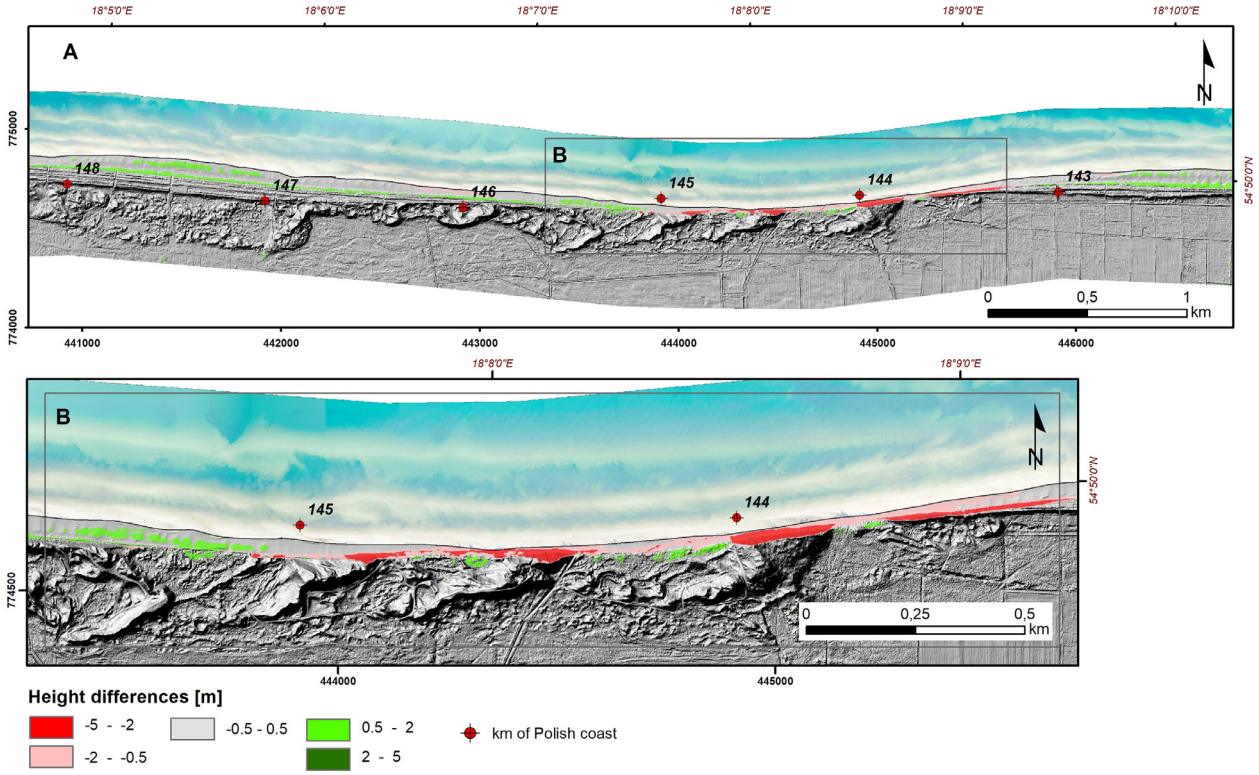

Figure 5 Multi-temporal DTM presenting the vertical change in beach and dune profiles between 2016 and 2020.

can be referred to as a "state of equilibrium" (Figure 4, Tables 2 and 3).

West of the erosional hot spot, i.e. west of km 145.6, the coast is characterised by the presence of a few local transition zones, i.e. points along the coast where local changes in erosion/accretion trends are observed. This is manifested by the oscillatory nature of changes. For instance, in the period 1875—1958, the average shoreline retreat was 20 m while the maximum shoreline retreat was up to 70 m, but in the same period, nearby areas experienced seaward shoreline migration (average value of 6 m and up to 30 m). While average and peak values of coastal erosion were lower between 1958 and 1980, with a shoreline retreat of 13 m (up to 22 m), average values of seaward accretion were 4 m with peak values up to 50 m. The period between 1980 and 2001 was characterised by seaward migration of the shoreline with an average of 32 m and maximum value of 50 m. The subsequent periods can be described as a state of equilibrium with a minor dominance of seaward shifts of the shoreline: 2001—2005 average 7 m, up to 25 m, 2005—2010 average 7 m, up to 43 m, 2010—2016 average 11 m, up to 37 m, 2016—2020 average 3 m, up to 26 m, while the erosion rate was as follows: 2001—2005 average 1 m, up to 20 m, 2005—2010 average 9 m, up to 29 m, 2010—2016 average 4 m, up to 28 m, 2016—2020 average 10 m, up to 33 m.

Although changes in the shoreline position within the eastern and western boundary zones of the erosional hot spot were relatively small and varied in time and space, it can be observed that accretion prevailed in the west and erosion prevailed in the east, with the erosional centre moving eastwards (Tables 2 and 3, Figure 4).

The above identification of the EHS and the two adjacent areas is clearly reflected in mapped vertical changes in the relief, i.e. changes in the volume of sediments in the inland part of the coastal zone. However, the western part of the EHS shows the opposite, vertical accretion. The central and eastern parts of the EHS are marked by decreased dune and beach height as well as reduced beach width (Figure 5). The beach was lowered by 0.5 to 1.5 m, but the most significant changes are observed within the remnant of parabolic dunes, up to 19 m above sea level (Figure 6). The reduction in height of the seaward slope of these dunes as well as on adjacent foredunes amounts to more than 2 m (Figure 5). In general, the beach and dunes in the western part of the EHS are in a state of equilibrium, with a local small increase in beach height (Figure 5). Importantly, these vertical changes indicate an eastward shift of the EHS.

The elevation changes outside the erosional hot spot, i.e. east of km 143.4 km and west of km 145.6, show that they are much more stable. In between small, sparse, isolated patches of fields with a negative trend of change from —0.5 to —2 m, positive trends in elevation between 0.5 to 2 m were also recorded and can be considered dominant. They are mainly located at the base of and within the dunes, but also on some parts of the beach.

5. Discussion

The average rate of coastal retreat during 145 years between 1875 and 2020 was not steady over time. During the first 83 years (1875—1958), the average shoreline retreat was only 0.3 m/yr (average rate measured from peak

Table 4 Shoreline retreat rates (pick and average) and area loss calculated for the "erosional hot spot".

Measured period	Maximum shorline erosion [m]	Average peak shoreline erosion rate [m/yr]	Net longshore average erosion [m]	Average shoreline erosion rate (calculated from longshore average erosion) [m/yr]	Area of net erosion [m^2]	Average rate of area loss [m^2/yr]
1875—1958	64	0.8	25	0.3	54591	658
1958—1980	64	2.9	14	0.6	30942	1406
1980 —2001	33	1.6	14	0.7	24574	1170
2001—2005	61	15.3	31	7.7	55744	13936
2005—2010	33	6.6	6	1.1	12441	2488
2010 —2016	42	7.0	21	3.5	45818	7636
2016—2020	31	7.8	13	3.2	28467	7117

Figure 6 Aerial view (towards the ESE) of the study area (photo by: M. Olkowicz, 2018). No foredune within the "hot spot"; visible: very narrow beach in front of the erosional undercut in the remains of the parabolic dune.

values was 0.8 m/yr) and was close to or even slightly lower than the average erosion rate of the Polish coast (e.g. Zawadzka, 1999). The shoreline retreat significantly accelerated in the second half of the 20th century, especially at the beginning of the 21st century. The rate of the shoreline retreat in the analysed six periods between 1958 and 2020 varied greatly from 0.6 to 7.7 m/yr (1.6 to 15.3 m/yr according to peak values) (Table 4). The most rapid coastal retreat, 7.7 m/yr (peak value up to 15.3 m/yr), occurred in a relatively short period between 2001 and 2005, which then slowed down to 3.5—3.2 m/yr (peak rates 6.6—7.8 m/yr), i.e. for the next 15 years remained clearly higher than before 2000. The sandy barrier coastal long-term retreat rate exceeding 5—10 m/yr is rarely reported worldwide (e.g. Eberhards and Saltupe, 1995; Eberhards et al., 2006; List et al., 1997; Nanson et al., 2022; Stachurska, 2012), thus the average value of 7.7 m/yr and average peak erosion rate 15.3 m/yr is unique.

The average erosion parameters are in very good correlation with the average rate of area loss (Figure 7). This demonstrates the validity of the described shoreline behaviour trends.

To answer the question about the cause of changes in the coastal retreat rate, we analysed trends in the variability of the rate of relative water level changes, changes in storminess as well as changes of sea-ice extent. Climatic oscillations on the scale of decades and centuries are potentially of high geomorphological importance. A range of geomorphological effects of such climatic oscillations have been recognised, i.e. coastal erosion (e.g. Viles and Goudie, 2003). The climate variability over the North Atlantic is known to be dominated by decadal-to-multidecadal fluctuations that have profound global and regional climate impacts (e.g. Börgel et al., 2020; Chafik et al., 2019; Knight et al., 2006; Peings and Magnusdottir, 2014), including the Baltic Sea and the surrounding areas (e.g.

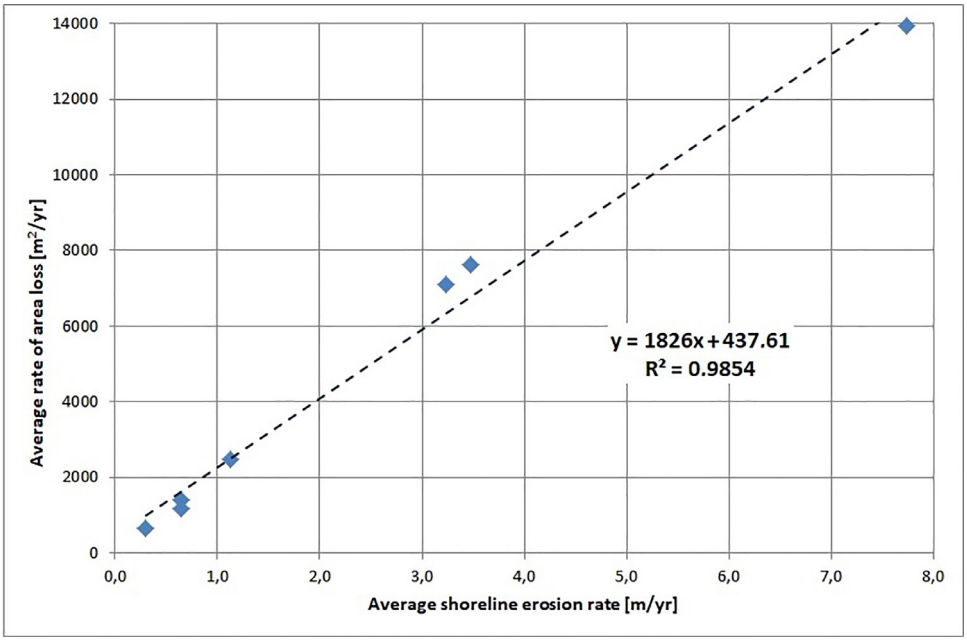

Figure 7 Correlations between average shoreline erosion rate (calculated from longshore average erosion) and average rate of area loss. The dashed blue line represents linear trend, the blue "diamonds" represents measured series.

Rutgersson et al., 2022; Slonosky et al., 2000). The North Atlantic Oscillation (NAO) and the Atlantic Multidecadal Oscillation (AMO), in particular, are two of the most prominent modes impacting the climate variability. The NAO index varies from days to decades. The long-term behaviour of the NAO is essentially irregular, and there is a large inter-annual to inter-decadal variability. The Atlantic Multidecadal Oscillation (AMO) has been identified as a coherent mode of natural variability occurring in the North Atlantic Ocean with an estimated period of 60—80 years (Rutgersson et al., 2022). NOA and AMO have a major impact on, among other features, sea level variability (e.g. Calafat et al., 2012, 2013; Chafik et al., 2019; Dangendorf et al., 2014) and changes in the frequency of storminess (e.g. Feser et al., 2015; Krueger et al., 2019). A positive high correlation coefficient of $\geq$ 0.5 for the NAO index, the maximum significant wave height Hs and the number of storms for Baltic Proper were identified for the period 1980—2015. A variability period of about 10—12 years was identified (Myslenkov et al., 2018). In summary, there has been considerable decadal and multidecadal variability in wind speed and direction for the last 200 years and correspondingly no clear indication of long-term trends in the frequency of storm surges and wave height (Bärring and Fortuniak, 2009; Feser et al., 2015; Rutgersson et al., 2014). Published trends in storm activity depend critically on the time analysed, data or the model used. Despite large decadal variations, a positive trend in the number of deep cyclones has been observed over the last six decades (Rutgersson et al., 2022). This is also recognised on the Polish coast, where an increasing trend in storm surge indicator values was observed in 1997—2008 (Stanisławczyk, 2012).

Storm surges have always been of interest to chroniclers and scientists (e.g. Dziadziuszko and Jednorał, 1996; Majewski, 1986, 1998; Rojecki, 1965; Sztobryn et al., 2005; Wiśniewski and Wolski, 2009; Wolski et al., 2014; Extreme Wind Storms Catalogue, 2022; List of European Windstorms, 2022). A review of literature and internet databases also indicates an increased number of storm surges on the Polish coast since 1980. The literature also contains information about frequent and severe storms occurring in the southern Baltic at the end of the 19th century and in the first decade of the 20th century (e.g. Majewski, 1998), although quantitative data from that period are scarce and not very accurate. The same is true for almost the entire 20th century, which was probably due to little interest in climate change at that time and only exceptionally catastrophic storms were recorded.

The average rate of water level rise according to the mareograph in Władysławowo, the nearest to the study area, in the period 1951—2015 was 2.04 mm/year. For the same period, the average rate in Gdańsk was 2.43 mm/yr (Kowalczyk, 2019). This slight discrepancy may be caused by differences in vertical ground movements. A much longer record of water level changes, starting from 1886, comes from Gdańsk (Figure 8). Trends in mean annual water level changes for corresponding periods are the same along the Polish coast, therefore we use the record from Gdańsk to analyse potential relationships between changes in the shoreline position, water level and storminess. The average rate of water level rise in Gdańsk in the period 1886—2021 according to a linear trend was 1.54 mm/yr, however, it varied strongly on multidecadal and decadal time scales (Figure 8).

These facts clearly indicate the underlying cause of the increased rate of coastal retreat starting in the second half of the 20th century. The changes in the coastal retreat rate (Table 3) correlate well with an increasing multidecadal trend in storm activity starting in the mid-1960s and continuing into the 1990s (Krueger et al., 2019), as well as the increasing storminess occurring over the decades 2000—2020 (Rutgersson et al., 2022; Stanisławczyk, 2012). During the

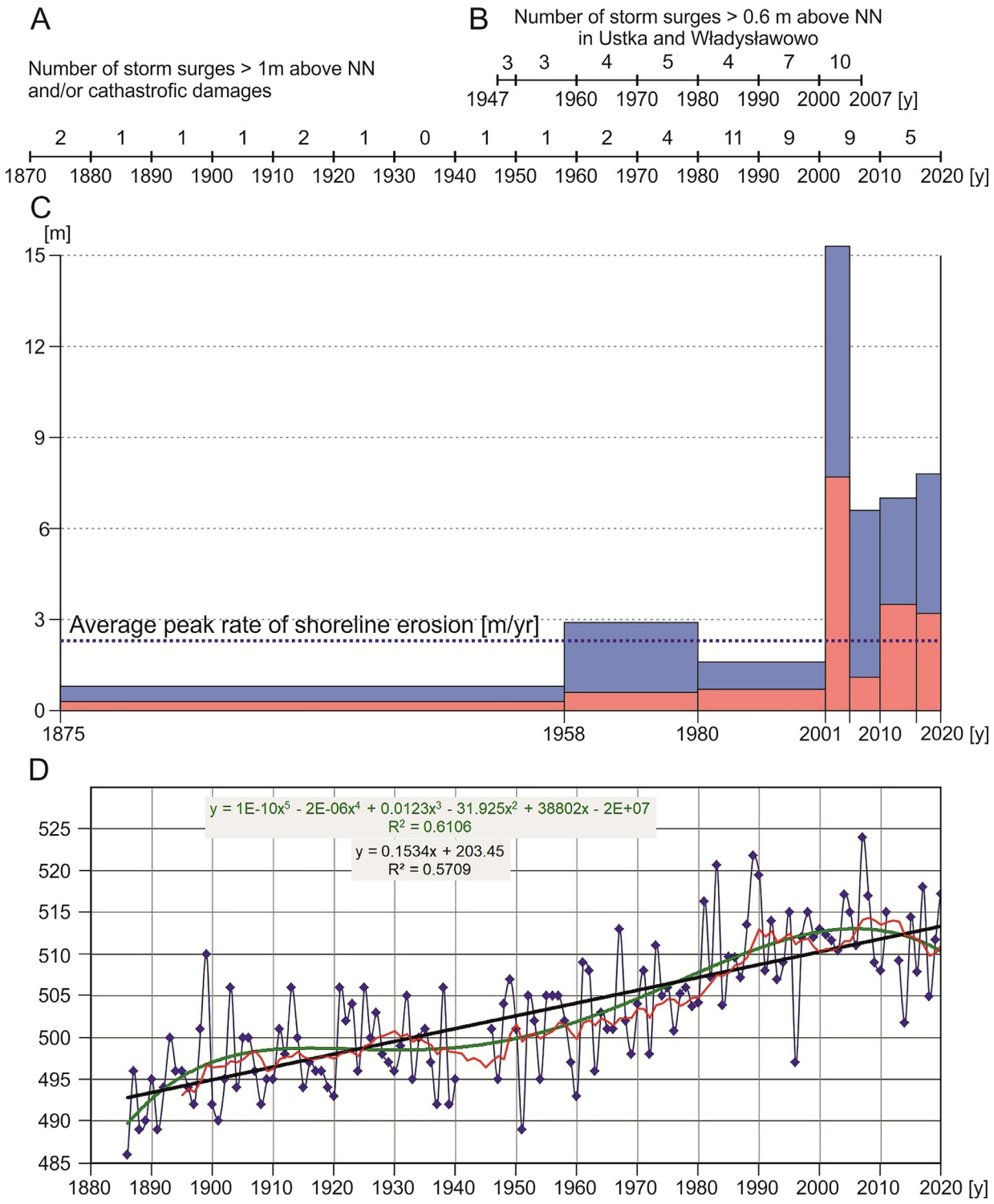

Figure 8 Erosion rate in relation to number of storms and sea level rise;
A — Number of storm surges > 1 m above NN and/or cathastrofic damages (according to Majewski (1986, 1998), Dziadziuszko and Jednorał (1996), Sztobryn et al. (2005), Extreme Wind Storms Catalogue (2022), List of European Windstorms (2022));
B — Number of storm surges > 0.6 m above NN in Ustka and Władysławowo
(according to Wiśniewski and Wolski (2009));
C — Rate of average shoreline retreat (pink bars) and average peak shoreline retreat (blue bars);
D — Annual average sea level changes according to the Gdańsk mareograph;
The black line represents the linear trend, the red line is the 10-year running average and the green line is the trend approximated by a 5-degree polynomial.

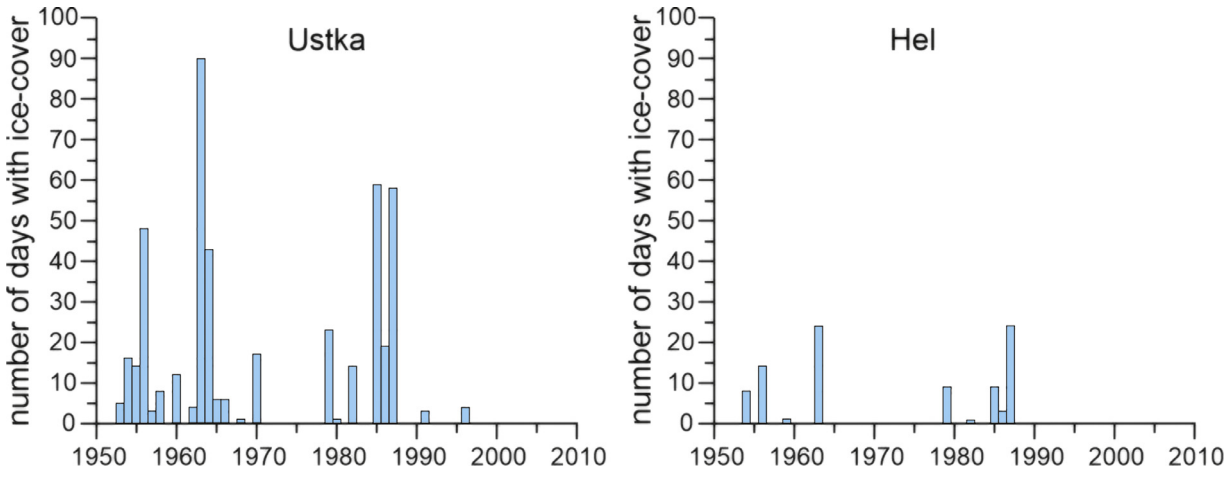

Figure 9 Ice-cover in Ustka and Hel, ports located west and east from discussed erosional hot spot (according to Sztobryn et al. (2012) — with changes).

same time, there were changes in decadal trends in water level changes (Figure 8). The highest rate of coastal retreat occurred between 2000 and 2005, when the NOA index was low (e.g. Krueger et al., 2019; Rutgersson et al., 2022) and the decadal trend of average sea level decreased (Figure 8), but there were several extremely severe storm surges, including in particular on 23 November 2004 (Elisabeth), 22 December 2004 (Rafael), and 9 January 2005 (Erwin-Gudrun), which caused catastrophic damage to the southern Baltic coast. For example, on December 22, 2004, during Storm Rafael, the height of the significant wave at the time was about 8.2 m, and the highest wave was estimated at a record 14 meters (https://obserwator.imgw.pl/wielkie-fale-na-baltyku/).

This means that NAO and AMO increased trends are of crucial importance for the rate of coastal retreat on the decadal and multidecadal time scales, while random extreme phenomena play an important role on a shorter time scale.

The increased rate of coastal retreat can also be explained by changes in sea ice cover, which is also one of the important factors suppressing surface waves and protecting shores against erosion by storm surges (Climate Change in the Baltic Sea, 2021). Maximum sea-ice extent of the Baltic Sea, duration of ice season and maximum thickness of level ice have been monitored regularly in the Baltic Sea since the late 19th century. All sea-ice observations demonstrated large inter-annual variations, but with a long-term, statistically significant trend to milder. Over the past 100 years, winters have become milder, the ice season shorter and the maximum ice extent has decreased and the period 1991—2020 was by far the mildest since ice conditions of 1720 (Meier et al., 2022). (e.g. Haapala et al., 2015, Meier et al., 2022). The interannual variability of the maximum ice extent of the Baltic Sea is owing to large-scale atmospheric circulation associated with the NAO. Greater ice extent occurs during negative phases of the NAO, while less ice extent occurs when the NAO is in a positive phase.

There has been a statistically significant decrease in the number of days with ice on the Polish coast in the period 1950-2010. Slightly less significant changes occur only in Ustka, while the smallest changes occur in Hel (Figure 9), i.e. in ports located west and east from discussed erosional hot spot. In the case of the southern Baltic, the correlation between the NAO index (averaged over 4 winter months) and sea-ice is relatively weak (—0.23). (Sztobryn et al., 2012). The number of days with sea ice in Ustka in the period 1950—2010 ranged from 0 to 90. Despite the aforementioned relatively weak correlation (Figure 9), the highest number of days (>20) with sea ice in Ustka occurred in 1956, 1963—1964, 1979 and 1985—1987, i.e. during the negative winter NAO index (https://commons.wikimedia.org/wiki/File:Winter-NAO-Index.svg). However, there was no sea-ice in Ustka (and on the beaches between Ustka and Hel) after 1996 despite occurrence of negative winter NAO index in 2000, 2003—2005, 2008—2010 and 2020, so declining and lack of ice cover increases the risk and severity of coastal erosion.

At the end of the 19th century and during the first decade of the 20th century, the level of storminess was high, compared to the multidecadal upward trend in storm activity starting in the mid-1960s and continuing into the 1990s (Krueger et al., 2019). At the same time, the rate of annual average sea level rise increased up to about 10 mm/year (Figure 8). Due to the high storminess and high rate of sea level rise, the range and rate of coastal retreat must have been high at that time. However, there are no data on the range of coastal retreats for that period. The calculated rate of shoreline retreat for the period 1875—1958 is only 0.8 m/year, which is even lower than the average rate for the entire analysed period (Table 3). This is most likely because storm activity has decreased since 1914. Although severe storms occurred after 1914, the storm surges did not exceed 1.5 m. Until 1995, only one storm (1941) was recorded, when the water level exceeded the average sea level by 1.5 m (Majewski, 1998). There was also the increase of extent of sea-ice around 1916—1929 and 1940—1943 (Meier et al., 2022; https://www.eea.europa.eu/data-and-maps/daviz/maximum-extent-of-ice-cover-3#tab-4186). During the 30 years between 1910 and 1940, the annual average sea level decreased and then increased very slowly until ca. 1980

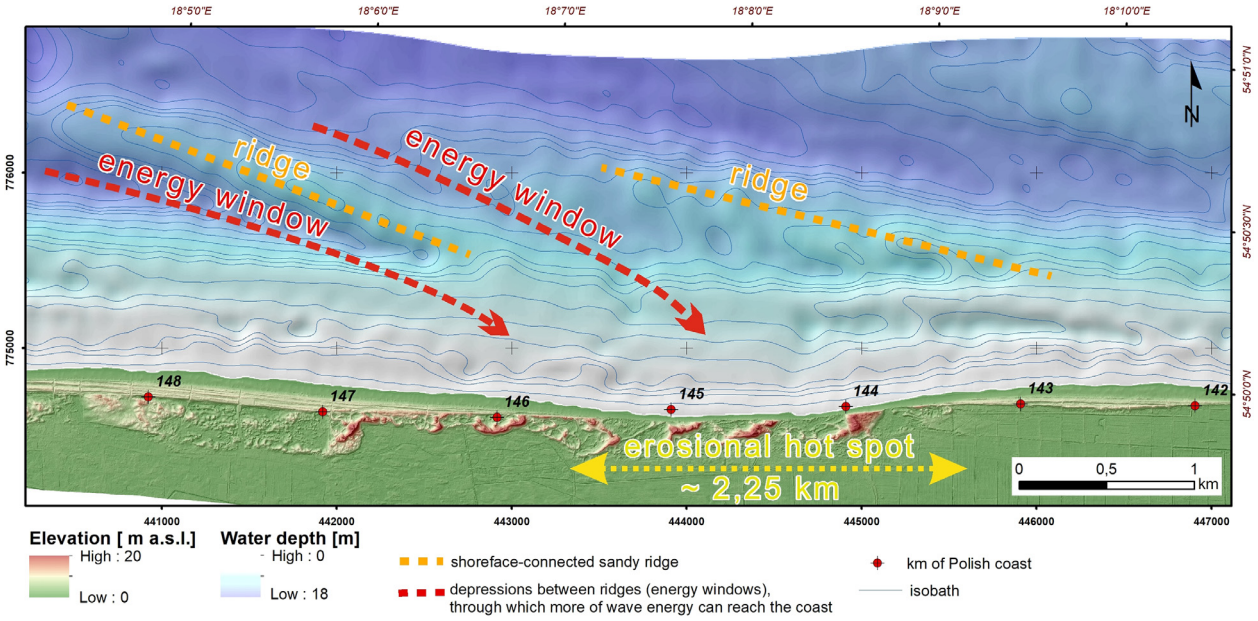

Figure 10 System of ridges and seabed depressions (energy windows) in the forefield of the erosional hot spot.

(Figure 8). As a result, the low coastal retreat rate calculated for the period 1875–1958 is most likely due to an averaging of changes from the periods of rapid coastal erosion (1875–1910) and the period of relative stabilisation (1910–1960). The discussed case of the erosion hot spot shows that the published data on the extent and rate of coastal retreat critically depend on the analysed period, and it is not always possible to clearly correlate the identified coastal erosion trends with the natural variability of the sea level and the frequency of storms.

According to the classification of erosional hot spots (Kraus and Galgano, 2001), the discussed hot spot can be classified as a type of translatory longshore sand wave (most probably) or a standing longshore sand wave with longshore dominant transport direction. The Translatory Longshore Sand Wave is indicated by the dominant (net) sediment transport direction from west to east (Szmytkiewicz et al., 2021), as well as greater accretion at the western boundaries and greater erosion at the eastern boundaries of the discussed hot spot (Table 2, Figures 4 and 5). If this is a Translatory Longshore Sand Wave, it cannot be classified as short/medium based on its duration (acc. to Kraus and Galgano, 2001; short = about a year; medium = about several years), as it has existed since the end of 19th century or at least since middle of 20th century. This discrepancy can be explained by the low offshore seabed dynamics of the tideless Baltic Sea, which is much lower than that known from tidal shelf seas and oceanic coasts. In such a case, the duration of the discussed hot spot is long-lasting, i.e. longer than the duration of a typical (e.g. investment) project, property ownership, or even longer, i.e. geologic time scale (Kraus and Galgano, 2001). The duration of the discussed EHS is longer than a century. Its lateral extent indicates that it is a local but most likely migratory phenomenon.

Consistent with the cause of erosion, the hot spot is associated with seasonal changes in wave climate over irregular offshore/nearshore topography and local wave focusing (Figure 10) (Bender and Dean, 2003). Seaward, behind the shoreface, in the vicinity of the discussed erosional hot spot there are seabed depressions between shoreface-connected sand ridges oriented obliquely to the shore which are a kind of “energy windows”, through which more wave energy can reach the coast.

With regard to the issue as to whether the discussed hot spot could have been predicted, we can state that the existing bathymetric and topographic data allow this, but these data were not available a few years ago, whereas the discussed erosional hot spot has existed for more than a century.

Since most of the published data on erosive hot spots comes from the coasts of high-energy tidal seas or ocean coasts, it can be assumed, based on the data presented above, that the idea of erosional hot spots can also be successfully applied to the coasts of nontidal and semi-enclosed intercontinental seas. However, the guidelines and some rules for classifying hot spots, especially in terms of its duration of existence should be modified due to lower energy levels.

6. Conclusions

The shoreline follows a sinusoidal course, with a positive amplitude corresponding to accretion and a negative amplitude to erosion. An extremely erosive trend (hot spot) is distinguished between 143 and 146 km of the coastline, with an increased rate of erosion observed from 2001. Since then, it has increased several times and has led to the erosion of dunes, the maximum height of which reaches 19 m above sea level. This is attributed to geological, geomorphological and hydrodynamical factors. The depressions between shoreface-connected sand ridges are “energy windows”, through which more wave energy can reach the coast. As a result, erosional embayments are formed onshore.

The main reason for accelerated coastal erosion during the recent decades are increased number of storms and decease extent of sea ice and decrease number of days with sea-ice. In addition to multidecadal and decadal climatic forcing, extraordinary events like storms in 2004—2005 played an important role in contributing to catastrophic changes on the coast in shorter periods.

According to the classification of erosional hot spots (Kraus and Galgano, 2001), the discussed hot spot can be classified as a type of translatory longshore sand waves, most likely with the dominant longshore direction of transport, and as indicated by the lateral extent, it is local but most likely advancing. Further research is required to fully address this question.

As for the cause of the erosional hot spot, it is related to seasonal changes in wave climate over irregular offshore/nearshore topography and local wave focusing.

In terms of duration, the hot spot in question is long lasting, i.e. lasted longer than the duration of i.a. a typical investment project, property ownership, or even longer (geologic time scale). The lifespan of the EHS is over one hundred years.

As for the question of whether the hot spot in question could have been predicted, we can argue that the existing bathymetric and topographic data allow this, but these data were not available a few years ago, whereas the hot spot has existed for more than a century.

Thus, multidecadal to decadal climate variability can trigger a pulse of hydrodynamic activity resulting in a complex coastal response. However, we have to remember that climate is not the only factor controlling the coastal processes, coastal geomorphology and geology is in many cases the determining factor.

The presented research allows us to conclude that the presented approach (EHS analyses) is also applicable to any barrier coast, including non-tidal basins.

Declaration of competing interest

The authors declare that they have no known competing financial interests or personal relationships that could have appeared to influence the work reported in this paper.

Acknowledgements

The authors express their gratitude to the Editor and Reviewers for their comments which helped to improve the article. The study presented may be considered as a contribution to EMODnet Geology project.

Funding

The authors disclose the receipt of the following financial support for research and the publication of this article: The data was collected under the project “4D cartography in the coastal zone of the southern Baltic Sea” financed by The National Fund for Environmental Protection and Water Management.

Data availability

LiDAR data (Digital Terrain Models), orthophotomaps are available via https://sipam.gov.pl/ and https://www.mediafire.com/folder/u95l9197wjsiv/Monitoring (property of Maritime Office). The topographic maps were obtained from the state geodetic resource under license conditions. The restrictions do not allow open sharing of the proprietary data used in this research, but data are available upon request made to the General Office of Geodesy and Cartography or partially via www.geoportal.gov.pl.

Authors contribution

Grzegorz Uścinowicz: conceptualization, methodology, writing — original draft preparation. Szymon Uścinowicz: conceptualization, text review. Tomasz Szarafin: methodology, software, visualization. Elżbieta Maszloch: writing — regional settings. Kamila Wirkus: writing — regional settings, editing.

References

Bärring, L., Fortuniak, K., 2009. Multi-indices analysis of southern Scandinavian storminess 1780—2005 and links to interdecadal variations in the NW Europe—North Sea region. Int. J. Climatol. 29, 373—384.

Börgel, F., Frauen, C., Neumann, T., Meier, H.E.M., 2020. The Atlantic Multidecadal Oscillation controls the impact of the North Atlantic Oscillation on North European climate. Environ. Res. Lett. 15 (10), 104025. https://doi.org/10.1088/1748-9326/aba925

Bender, C.J., Dean, R.G., 2003. Wave field modification by bathymetric anomalies and resulting shoreline changes: a review with recent results. Coast. Eng. 49 (1—2), 125—153.

Benedet, L., Finkl, C.W., Hartog, W.M., 2007. Processes Controlling Development of Erosional Hot Spots on a Beach Nourishment Project. J. Coast. Res. 231, 33—48. https://doi.org/10.2112/06-0706.1

Bridges, M.H., 1995. Analysis of the processes creating erosional hot spots in beach nourishment projects. Coastal & Oceanographic Engineering Program. University of Florida, Gainesville, FL, 135.

Calafat, F., Chambers, D., Tsimplis, M., 2012. Mechanisms of decadal sea level variability in the eastern North Atlantic and the Mediterranean Sea. J. Geophys. Res. Ocean. 117, C09022. https://doi.org/10.1029/2012JC008285

Calafat, F., Chambers, D., Tsimplis, M., 2013. Inter-annual to decadal sea-level variability in the coastal zones of the Norwegian and Siberian Seas: The role of atmospheric forcing. J. Geophys. Res. Ocean. 118 (3), 1287—1301. https://doi.org/10.1002/jgrc.20106

Chafik, L., Nilsen, J.E.Ø., Dangendorf, S., Reverdin, G., Frederikse, T., 2019. North Atlantic Ocean circulation and decadal sea level change during the altimetry era. Sci. Rep. 9, 1041. https://doi.org/10.1038/s41598-018-37603-69

Climate Change in the Baltic Sea, 2021. Fact Sheet. [in:] Baltic Sea Environment Proceedings n°180. HELCOM/Baltic Earth, 2021.

Dangendorf, S., Calafat, F.M., Arns, A., Wahl, T., Haigh, I.D., Jensen, J., 2014. Mean sea level variability in the North Sea: Processes and implications. J. Geophys. Res. Ocean. 119, 6820—6841. https://doi.org/10.1002/2014JC009901

Dean, R.G., Liotta, R., Simon, G., 1999. Erosional hot spots. Coastal and Oceanographic Engineering Program, Technical Report UFL/COEL-99/021, University of Florida, Gainesville, 60 pp.

Deng, J., Harff, J., Zhang, W., Schneider, R., Dudzińska-Nowak, J., Terefenko, P., Giza, A., Furmańczyk, K., 2017. The dynamic equilibrium shore model for the reconstruction and future projection of coastal morphodynamics. [in:] Harff, J., Furmańczyk, K., von Storch, H. (Eds.), Coastline Changes of the Baltic Sea From South to East, Past and Future Projection. Coastal Research Library 19, Springer, 87—106.

Dziadziuszko, Z., Jednorał, T., 1996. Zagrożenia powodziowe powodowane spiętrzeniami sztormowymi u brzegów Bałtyku i Zalewu Wiślanego, [Flood hazard caused storm surges off the coast of the Baltic Sea and the Vistula Lagoon]. Wiad. IMGW. 19 (3), 123—133.

Eberhards, G., Saltupe, B., 1995. Accelerated coastal erosion — Implications for Latvia. Baltica. 9, 16—28.

Eberhards, G., Lapinskis, J., Saltupe, B., 2006. Hurricane Erwin 2005 coastal erosion in Latvia. Baltica 19, 16—28.

Esteves, L.S., Finkl, C.W., 1998. The Problem of Critically Eroded Areas (CEA): An Evaluation of Florida Beaches. J. Coast. Res. 11—18. http://www.jstor.org/stable/25736114

Extreme Wind Storms Catalogue. http://www.europeanwindstorms.org/cgi-bin/storms/storms.cgiT (accessed May 2022).

Feser, F., Barcikowsk, M., Krueger, O., Schenk, F., Weisseaand, R., Xiae, L., 2015. Storminess over the North Atlantic and northwestern Europe —A review. Q. J. R. Meteorol. Soc. 141, 350—382. https://doi.org/10.1002/qj.2364

Furmańczyk, K., Musielak, S., 1999. Circulation systems of the coastal zone and their role in south Baltic morphodynamic of the coast. Circulation systems of the coastal zone and their role in the South Baltic morphodynamics of the coast. Quart. Stud. Pol. Spec. Issue, 91—94.

Furmańczyk, K., Musielak, S., 2002. Importent features of coastal dynamics in Poland: „Nodal Points" and „Gates. [in:] Schernewski, G., Schiwer, U. (Eds.), Baltic coastal ecosystems. Structure, Function and Coastal Zone Management. Springer-Verlag, Berlin, Heidelberg, New York, 141—147. https://doi.org/10.1007/978-3-662-04769-9

Furmańczyk, K., 1994. Współczesny rozwój strefy brzegowej morza bezpływowego w świetle badań teledetekcyjnych [Present coastal zone development of the tide less sea in light of the South Baltic Sea coast remote sensing investigating], 161. Uniwersytet Szczeciński Rozprawy I Studia T, 179 CCXXXV, (in Polish with English sumary).

Galgano, F.A., 2007. Types and causes of beach erosion anomaly areas in the U.S. east coast barrier island system: stabilized tidal inlets. Middle States Geogr, 40, 158—170.

Haapala, J.J., Ronkainen, I., Schmelzer, N., Sztobryn, M.The BACC II Author Team, 2015. Recent Change—Sea Ice. Second Assessment of Climate Change for the Baltic Sea Basin. Regional Climate Studies. Springer, Cham. https://doi.org/10.1007/978-3-319-16006-1_8

HELCOM, 2007. Climate change in the Baltic Sea area — HELCOM thematic assessment in 2007. Baltic Sea Environ. Proc. 111, 49.

HELCOM, 2013. Climate change in the Baltic Sea area — HELCOM thematic assessment in 2013. Baltic Sea Environ. Proc. 137, 66.

Knight, J.R., Folland, C.K., Scaife, A.A., 2006. Climate impacts of the Atlantic Multidecadal Oscillation. Geophys. Res. Lett. 33, L17706. https://doi.org/10.1029/2006GL026242

Kowalczyk, K., 2019. Changes in mean sea level on the Polish coast of the Baltic Sea based on tide gauge data from the years 1811—2015. Acta Geodyn. Geomater. 16 (2), 195—209.

Kraus, N.C., Galgano, F.A., 2001. Beach erosional hot spots: types, causes, and solutions. Coastal and Hydraulics Engineering Technical Note CHETN-II-44. U.S. Army Engineer Research and Development Center, Vicksburg, MS, 1—17.

Krueger, O., Feser, F., Weisse, R., 2019. Northeast Atlantic Storm Activity and Its Uncertainty from the Late Nineteenth to the Twenty-First Century. J. Climate 32, 1919—1931. https://doi.org/10.1175/JCLI-D-18-0505.1

List, J.H., Sallenger, A.H., Hansen, M.E., Jaffe, B.E., 1997. Accelerated relative sea-level rise and rapid coastal erosion: testing a causal relationship for the Louisiana barrier islands. Mar. Geol. 140 (1997), 347—365. https://doi.org/10.1016/S0025-3227(97)00035-2

List of European windstorms. https://www.wikiwand.com/en/List_of_European_windstorms# (accessed May 2022).

Majewski, A., 1986. Skrajne wahania poziomu wody u polskich wybrzeży Bałtyku, [Extreme fluctuations of the water level on the Polish Baltic coast]. Inżynieria Morska 2, 46—50.

Majewski, A., 1998. Największe wezbrania wód u południowych brzegów Morza Bałtyckiego, [The highest storm surges along the southern coast of the Baltic Sea]. Wiad. IMGW. 21 (2), 81—98.

Meier, H.E.M., Kniebusch, M., Dieterich, C., Gröger, M., Zorita, E., Elmgren, R., Myrberg, K., Ahola, M.P., Bartosova, A., Bonsdorff, E., Börgel, F., Capell, R., Carlén, I., Carlund, T., Carstensen, J., Christensen, O.B., Dierschke, V., Frauen, C., Frederiksen, M., Gaget, E., Galatius, A., Haapala, J.J., Halkka, A., Hugelius, G., Hünicke, B., Jaagus, J., Jüssi, M., Käyhkö, J., Kirchner, N., Kjellström, E., Kulinski, K., Lehmann, A., Lindström, G., May, W., Miller, P.A., Mohrholz, V., Müller-Karulis, B., Pavón-Jordán, D., Quante, M., Reckermann, M., Rutgersson, A., Savchuk, O.P., Stendel, M., Tuomi, L., Viitasalo, M., Weisse, R., Zhang, W., 2022. Climate change in the Baltic Sea region: a summary. Earth Syst. Dynam. 13, 457—593. https://doi.org/10.5194/esd-13-457-2022

Michałowska, K., Głowienka, E., 2022. Multi-temporal analysis of changes of the southern part of the Baltic Sea coast using aerial remote sensing data. Remote Sens. 14, 1212. https://doi.org/10.3390/rs14051212

Moskalewicz, D., 2016. Torfowiska Mierzei i Niziny Karwieńskiej potencjalnym archiwum ekstremalnych zalewów sztormowych (The peatlands of the Karwia Barrier and Karwia Lowland as a potential archive of extreme storm floods). Acta Geogr. Lodz., 105, 141—148.

Musielak, S., Furmańczyk, K., Bugajny, N., 2017. Factors and processes forming the Polish Southern Baltic sea coast on various temporal and spatial scale. [in:] Harff, J., Furmańczyk, K., von Storch, H. (Eds.), Coastline Changes of the Baltic Sea From South to East, Past and Future Projection. Coastal Research Library 19, Springer, 69—85.

Myslenkov, S., Medvedeva, A., Arkhipkin, V., Markina, M., Surkova, G., Krylov, A., Dobrolyubov, S., Zilitinkevich, S., Koltermann, P., 2018. Long-term statistics of storms in the Baltic, Barents and White Seas and their future climate projections. Geogr. Environ. Sustain. 11 (1), 93—112. https://doi.org/10.24057/2071-9388-2018-11-1-93-112

Nanson, R., Bishop-Taylor, R., Sagar, S., Lymburner, L., 2022. Geomorphic insights into Australia's coastal change using a national dataset derived from the multi-decadal Landsat archive. Estuar. Coast. Shelf Sci. 265, 107712. https://doi.org/10.1016/j.ecss.2021.107712

Ostrowski, R., Schönhofer, J., Szmytkiewicz, P., 2016. South Baltic representative coastal field surveys, including monitoring at the Coastal Research Station in Lubiatowo. Poland. J. Marine Syst. 162, 89—97. https://doi.org/10.1016/j.jmarsys.2015.10.006

Peings, Y., Magnusdottir, G., 2014. Forcing of the wintertime atmospheric circulation by the multidecadal fluctuations of the North Atlantic ocean. Environ. Res. Lett. 9, 034018.

Pruszak, Z., Ostrowski, R., Schönhofer, J., 2011. Variability and correlations of shoreline and dunes on the southern Baltic coast (CRS Lubiatowo, Poland). Oceanologia 53 (1), 97—120. https://doi.org/10.5697/oc.53-1.097

Rojecki, A (Ed.), 1965. Wyjątki ze źródeł historycznych o nadzwyczajnych zjawiskach hydrologiczno-meteorologicznych na ziemiach polskich w wiekach od X do XVI. Wydawnictwa Komunikacji i Łączności, Warszawa.

Rutgersson, A., Jaagus, J., Schenk, F., Stendel, M., 2014. Observed changes and variability of atmospheric parameters in the Baltic Sea region during the last 200 years. Clim. Res. 61, 177—190. https://doi.org/10.3354/cr01244

Rutgersson, A., Kjellström, E., Haapala, J., Stendel, M., Danilovich, I., Drews, M., Jylhä, K., Kujala, P., Larsén, X.G., Halsnæs, K., Lehtonen, I., Luomaranta, A., Nilsson, E., Olsson, T., Särkkä, J., Tuomi, L., Wasmund, N., 2022. Natural hazards and extreme events in the Baltic Sea region. Earth Syst. Dynam. 13, 251—301. https://doi.org/10.5194/esd-13-251-2022

Slonosky, V.C., Jones, P.D., Davies, T.D., 2000. Variability of the surface atmospheric circulation over Europe, 1774—1995. Int. J. Climatol. 20, 1875—1897.

Stachurska, B., 2012. Analiza zmian położenia brzegu odmorskiej strony Półwyspu Helskiego na podstawie zdjęć lotniczych z lat 1947—1991. Inżynieria Morska i Geotechnika 4, 542—553.

Stanisławczyk, I., 2012. Storm-surges Indicator for the Polish Baltic Coast. TransNav — Int. J. Nav. Archit. Ocean Eng. 6 (1), 123—129.

Subotowicz, W., 1991. Ochrona brzegu klifowego na odcinku Jastrzębia Góra — Rozewie. Inżynieria morska i geotechnika 4, 143—145, (in Polish).

Subotowicz, W., 1995. Transformation of the cliff coast in Poland. J. Coast. Res. 22, 5—62.

Szmytkiewicz, P., Szmytkiewicz, M., Uścinowicz, G., 2021. Lithodynamic processes along the seashore in the area of planned nuclear power plant construction: A case study on Lubiatowo at Poland. Energies 14 (6), 1636. https://doi.org/10.3390/en14061636

Sztobryn, M., Stigge, H.J., Wielbińska, D., Weidig, B., Stanisławczyk, I., Kańska, A., Krzysztofik, K., Kowalska, B., Letkiewicz, B., Mykita, M., 2005. Storm surges in the southern Baltic (western and central parts), Rep. No. 39, Ber. Bundesamt für Seeschifffahrt und Hydrographie (BSH), Hamburg, Rostock, 74 pp.

Sztobryn, M., Wójcik, R., Miętus, M., 2012. Występowanie zlodzenia na Bałtyku — stan obecny i spodziewane zmiany w przyszłości. [in:] Jakusik, E., Wibig, J. (Eds.), Warunki klimatyczne i oceanograficzne w Polsce i na Bałtyku Południowym. Spodziewane zmiany i wytyczne do opracowania strategii adaptacyjnych w gospodarce krajowej: Występowanie zlodzenia na Bałtyku — stan obecny i spodziewane zmiany w przyszłości. Instytut Meteorologii i Gospodarki Wodnej, Warszawa, 189—215.

Terefenko, P., Paprotny, D., Giza, A., Morales-Nápoles, O., Kubicki, A., Walczakiewicz, Sz., 2019. Monitoring Cliff Erosion with LiDAR Surveys and Bayesian Network-based Data Analysis. Remote Sens. 11 (7), 843. https://doi.org/10.3390/rs11070843

Uścinowicz, G., Szarafin, T., 2018. Short-term prognosis of development of barrier-type coasts (Southern BalticSea). Ocean Coast. Manage. 165, 258—267. https://doi.org/10.1016/j.ocecoaman.2018.08.033

Uścinowicz, S.Z., Zachowicz, J., Graniczny, M., Dobracki, R., 2004. Geological structure of the southern Baltic coast and related hazards. Polish Geological Institute Special Papers 15, 61—68.

Uścinowicz, G, Jurys, L, Szarafin, T., 2017. The development of unconsolidated sedimentary coastal cliffs (Pobrzeże Kaszubskie, Northern Poland). Geol. Q. 61 (2), 491—501. https://doi.org/10.7306/gq.1351

Uścinowicz, G., Szarafin, T., Pączek, U., Lidzbarski, M., Tarnawska, E., 2021. Geohazard assessment of the coastal zone — the case of the southern Baltic Sea. Geol. Q. 65 (5). https://doi.org/10.7306/gq.1576

Viles, H.A., Goudie, A.S., 2003. Interannual, decadal and multidecadal scale climatic variability and geomorphology. Earth Sci. Rev. 61, 105—131.

Wiśniewski, B., Wolski, T., 2009. Katalogi wezbrań i obniżeń sztormowych poziomów morza oraz ekstremalne poziomy wód na polskim wybrzeżu, [Catalogues of storm-generated sea level surges and falls and extreme water levels on the Polish coast]. Wyd. AM, Szczecin.

Wolski, T., Wiśniewski, B., Giza, A., Kowalewska-Kalkowska, H., Boman, H., Grabbi-Kaiv, S., Hammarklint, T., Holfort, J., Lydeikaite, Ž., 2014. Extreme sea levels at selected stations on the Baltic Sea coast. Oceanologia 56 (2), 259—290. https://doi.org/10.5697/oc.56-2.259

Zawadzka, E., 1999. Tendencje rozwojowe polskich brzegów Bałtyku południowego [Development tendencies of the Polish shores of the southern Baltic Sea]. Gdańskie Towarzystwo Naukowe, Gdańsk, (in Polish with English summary).

Zawadzka, E., 2012. Morfodynamika brzegów wydmowych południowego Bałtyku. [Morphodynamics of the southern Baltic dune coasts]. Wydawnictwo Uniwersytetu Gdańskiego, Gdańsk, (in Polish with English summary).

Zawadzka-Kahlau, E., 1999. Trends in southern Baltic coast development during the last hundred years. Peribalticum 7, 115—136.